

Modes of Free Vibrations of
Cracked Beams

M. H. Shen
Graduate Student

C. Pierre
Assistant Professor

April 1986

#UM-MEAM-86-37

SUMMARY

A FINITE ELEMENT APPROACH IS PRESENTED WHICH MAKES IT POSSIBLE TO PREDICT THE CHANGES IN THE FIRST FEW EIGENFREQUENCIES, EIGENMODES DUE TO CRACKS (PAIRS, OR SINGLE OPEN CRACKS). EIGHT NODES ISOPERAMATRIC ELEMENT IS USED TO MODEL ACROSS THE THICKNESS OF THE BEAM (RECTANGULAR CROSS-SECTION). SOME EXPERIMENTS ON BEAMS CONTAINING CUTS TO SIMULATE CRACKS ARE BRIEFLY DESCRIBED. THE CHANGE IN THE FIRST NATURAL FREQUENCY WITH CRACK DEPTH IS MATCHED CLOSELY BY THE PRESENT FINITE ELEMENT APPROACH. THEORETICAL PREDICTIONS ARE ALSO MADE AND COMPARED TO EXPERIMENTAL AND FINITE ELEMENT RESULTS. IN THE THEORETICAL FORMULATIONS THERE IS A PARAMETER α WHICH MAY BE DETERMINED FROM EXPERIMENTAL RESULTS. THEREFORE, FOR A SPEIFIC CRACK DEPTH , THIS PARAMETER CAN ALSO BE EVALUATED BY FINITE ELEMENT METHOD TO IMPROVE THE THEORETICAL SOLUTIONS. SEVERAL DIFFERENT KINDS OF SINGULAR ELEMENTS ARE CONSIDERED AND DISCUSSED FOR FUTURE STUDIES.

TABLE OF CONTENTS

CHAPTERS		Pages
CHAPTER 1	INTRODUCTION.....	1
CHAPTER 2	CRACKED BERNOULLI-EULER BEAM THEORY.....	3
CHAPTER 3	FINITE ELEMENT FORMULATION	
	3-1 Co-Ordinate Systems.....	8
	3-2 Elastic Element Properties.....	8
	3-3 Crack Tip Element.....	11
	3-4 Consistent Mass Matrix.....	15
CHAPTER 4	RESULTS AND DISCUSSION.....	18
CHAPTER 5	CONCLUSIONS AND SUGGESTIONS FOR FUTURE RESEARCH.....	38
APPENDIX:	FINITE ELEMENT PROGRAM.....	44

CHAPTER 1 INTRODUCTION

The dynamical behavior of structures containing cracks is a subject of considerable current interest in the light of potential developments in automatic monitoring of structural integrity. The influence on the eigenfrequencies and eigenmodes of changes in the geometry (cracks) of a structure (beam) are in many respects important to know.

A crack in a structural member introduces a local flexibility which is a function of the crack depth. This flexibility changes the dynamic behaviour of the system and its stability characteristics.

The effect of the local flexibility of a cracked column upon its buckling load was studied by Liebowitz et al. [1,2] and Okamura [3]. These authors identified the compliance of a cracked column to a bending moment. Rice and Levy [4] recognized the coupling between bending and extensional compliance of a cracked column in compression.

The effect of cracks upon the dynamical behavior of cracked beams was studied by Dimarogonas [5] and Chondros and Dimarogonas [6]. They observed the local flexibility of the shaft due to the crack and gave an analytical expression for the crack local flexibility in relation to the crack depth, and also showed the influence of the crack upon the dynamics response of the rotor.

Very little analytical work and experimental work has been done previously on vibration problems. One of the important recent related research is described by Christides and Barr [7].

They derived the differential equation and associated boundary conditions for a nominally uniform Bernoulli-Euler beam containing one or more pairs of symmetric "open" cracks. The pairs of cracks are taken to be normal to the beam's axis and to be symmetrical about the plane of bending. The reason for this restriction on crack geometry is to hold the particular symmetry associated with bending motion. The reason for specifying an "open" crack is to avoid complexities which result from the nonlinear characteristics presented by a crack which can open and close. The equation of motion they derived was not solved directly, but the Rayleigh-Ritz method was used to obtain an estimate of the drop in the fundamental frequency of a simply supported beam in the presence of a mid-span crack. Theoretical results was then obtained by substituting a dimensionless parameter α which was evaluated by experimental tests.

A finite element approach for calculating the first few eigenfrequencies and eigenmodes of cracked beams is presented in this term paper. Eight nodes isoparametric element is used to model across the thickness of the beam. Since there is no geometrical assumptions for the finite element formulation the results obtained by finite element method are found to agree very well with the results from the results from the experimental test performed by Christides and Barr [7]. Therefore, in Barr's paper, the parameter α which had to be determined from experimental results can also be determined less expensively by present finite element approach.

In order to make clear comparison, theory for the cracked Bernoulli-Euler beam is outlined in the next section.

CHAPTER 2 CRACKED BERNOULLI-EULER BEAM THEORY

If displacement components are written as u_i strain components as γ_{ij} and stress components as τ_{ij} with $i, j=1, 2, 3$ referring to cartesian axes x, y, z , then the extended Hu-Washizu [8,9,10] variational principle states that for arbitrary independent variations δu_i , $\delta \gamma_{ij}$, $\delta \tau_{ij}$, and δp_i .

$$\int_V \{ [\tau_{ij} + F_i - \rho \dot{p}_i] \delta u_i + [\tau_{ij} - W_{,ij}] \delta \gamma_{ij} + [\gamma_{ij} - (1 - 1/2 \delta_{ij})(u_{ij} + u_{ji})] \delta \tau_{ij} + [\rho \dot{u}_i - T_{,pi}] \delta p_i \} dV + \dots (1)$$

$$\int_{S_r} [\bar{g}_i - g_i] \delta u_i dS + \int_{S_u} [u_i - \bar{u}_i] \delta g_i dS = 0$$

In this equation $W(\gamma_{ij})$ is the strain energy density function, ρ is the density, F_i and g_i are, respectively, the body forces and the surface tractions, V is the total volume of the system and S its external surface. The overbared quantities \bar{g}_i and \bar{u}_i denote the prescribed values of the surface tractions and the surface displacements, respectively. The former acts over the surface S_p and the latter over S_u . S_v and S_p together make up the total surface.

The introduction of cracks will lead to changes in the stress and strain distributions in the vicinity of the cracked section. It is known that near the crack tip there are large stress concentrations and disturbed and all components of stress are likely to be non-zero. The change in stress and strain distribution near the crack are brought in by using a function $f(x, z)$ which has its maximum value at the tip of the crack and which decays with distance from the cracked section.

The assumptions made following notation for a nominally uniform beam in the absence of body forces,

$$\begin{aligned}
u_1 &= u = -z w' & u_2 &= v = 0 & u_3 &= w = w(x, t) \\
p_x &= 0 & p_y &= 0 & p_z &= P(x, t) \\
\gamma_{xx} &= [-z + f(x, z)] S(x, t) \\
\gamma_{yy} &= \gamma_{zz} = -\nu \gamma_{xx} & & & & \dots\dots\dots (2) \\
\gamma_{xy} &= \gamma_{yz} = \gamma_{xz} = 0 \\
\tau_{xx} &= [-z + f(x, z)] T(x, t) & \tau_{xz} &= \tau_{xz} (x, z, t) \\
\tau_{yy} &= \tau_{zz} = \tau_{xy} = \tau_{yz} = 0 \\
F_x &= F_y = F_z = 0
\end{aligned}$$

These assumptions can now be substituted in the general equation (1) and independent variations of the unknown w, p, S and T are considered. From the expression for δw of the equation (1) after substituted above assumptions yield the system's equation of motion.

$$\begin{aligned}
&E(I-K) Qw'' + 2E[Q'(I-K) - K'Q] w'''' + E[Q''(I-K) - 2K'Q' - K''Q] w'' \\
&+ \rho A \ddot{w} = 0 \quad \dots\dots\dots (3)
\end{aligned}$$

The boundary conditions appropriate to equation (3) are listed as follows: (for example for a cantilever beam).

$$\begin{aligned}
w = 0 & \quad w' = 0 & \text{at } x = 0 \\
(K - I) T = 0 & \quad , \quad (I - K) T' - K' T = 0 & \text{at } x=1
\end{aligned}$$

If it is assumed in the first place the cracks occur in symmetric pairs one from the upper surface z = -d of the beam and the other from its lower surface z = d, both at the same value of x. A typical situation is shown in Figure 1.

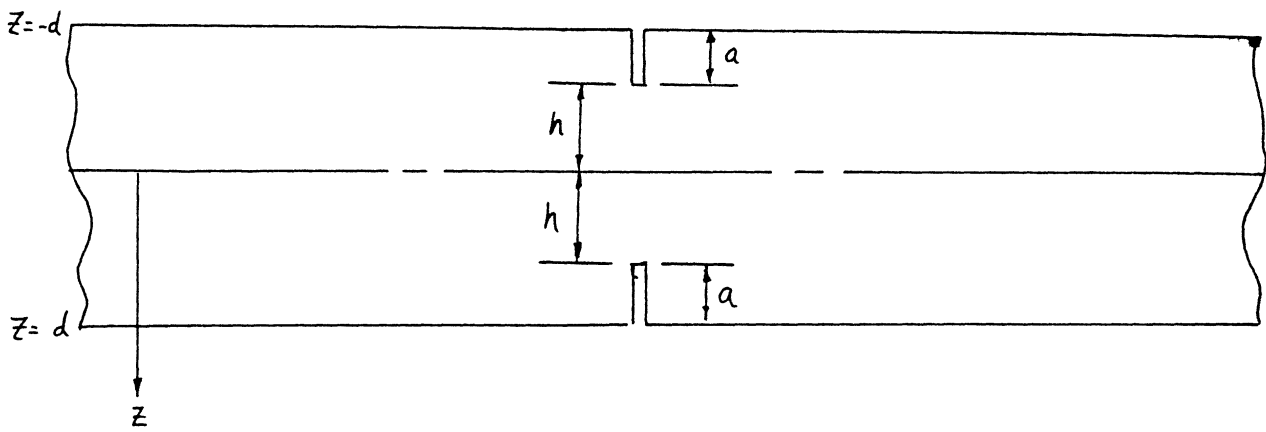


Figure 1 Typical symmetric crack geometry.

Thus, taking the crack to be at the position $x = 1/2$, the function $f(x,z)$ occurring in the stress distribution τ_{xx} is taken in the form

$$f(x,z) = [z - m z H(h - |z|)] \exp (-\alpha |x - 1/2| / d) \dots \dots \dots (4)$$

where H is a unit step function at $z=h$ and $m=(I/I_r)$

Where α is a positive non-dimensional constant which may be determined from experimental results. The use of $|x - 1/2|$ gives a symmetric decay on either side of the crack.

Using equation (4), the stress distribution can be written in a general way for the case in which the beam has symmetric crack at mid-span $x=1/2$, thus,

$$\tau_{xx}(x,z,t) = \{ - z + [z - m z H(h - |z|)] \exp(-\alpha|x - 1/2| / d) \} T(x,t) \dots (5)$$

On the case of a beam of rectangular section of depth $2d$ and breadth $2b$ with a symmetric pair of cracks at mid-span $x=1/2$. The constants I , I_r , K , L , Q and m of equations (3), (4), and (5) can be evaluated. They are found to be

$$I = 4 b d^3 / 3, I_r = 4 b h^3 / 3, m = (d/h)^3, K = 0$$

and

$$L = C I \exp(-2\alpha |x - 1/2| / d) \text{ where } C = (m - 1)$$

also

$$Q = [1 + C \exp(-2\alpha |x - 1/2| / d)]^{-1} \dots\dots\dots (6)$$

The equation of motion of the unloaded beam from equation (3) is

$$E I Q w'''' + 2 E I Q' w'''' + E I Q'' w'' + A w = 0 \dots\dots\dots (7)$$

This equation can be approached most easily analytically by using the Rayleigh-Ritz method. The Rayleigh quotient associated with equation (7) can be written in the form

$$(f_c / f_{BE})^2 = (1/\pi)^4 \int_0^1 Q(W'')^2 dx / \int_0^1 W^2 dx \dots\dots\dots (8)$$

where f_c is the natural frequency of the cracked beam, f_{BE} is the Bernoulli-Euler frequency of the uncracked beam and $W(x)$ is an assumed shape function.

For the first mode of a simply supported beam the shape function is taken (for $0 < x < 1/2$) as

$$W(x) = \sin(\pi x/l) + k \{ (x/l) - [4(x/l)^3 / 3] \} \dots\dots\dots (9)$$

substituting equation (9) in equation (8) results in

$$(f_c / f_{BE})^2 = \frac{X1 + (16 X2 k / \pi^2) + (64 X3 k^2 / \pi^4)}{0.25 + (16k/\pi^2) + 0.02698 k} \dots\dots (10)$$

where $X1$, $X2$, and $X3$ are the integrals

$$X_1 = \int_0^{1/2} Q \cos \pi r \, dr, \quad X_2 = \int_0^{1/2} (1/2 - r) Q \cos \pi r \, dr$$

.....(11)

$$X_3 = \int_0^{1/2} (1/2 - r)^2 Q \, dr$$

In the following chapter, I will outline the development of the crack finite element and obtain complete formulae for the system's equation of motion.

CHAPTER 3 FINITE ELEMENT FORMULATION

The finite element method has been proven to be an extremely powerful tool for obtaining the solution to structural problems involving complex geometries, arbitrary loadings and rather general material properties. In the present term project, eight nodes quadrilateral element is used to model across the thickness of the beam.

3 - 1 Co-Ordinate Systems

The geometriy of an arbitrary eight-node quadrilateral element is shown in Figure 2. The global coordinates system is x, y and local or element coordinates are given by s, t .

3 - 2 Elastic Element Properties

In the standard formulation of plane stress or strain the stiffness matrix is given by

$$[k] = \iint [B]^T [D] [B] dx dy \dots\dots\dots(12)$$

in which [B] is the matrix defining the strains in terms of the nodal displacement and [D] is the elasticity matrix which relates to the strains. The strain matrix is given by

$$\begin{matrix}
\{ \epsilon \} = & \begin{Bmatrix} u_{,x} \\ u_{,y} \\ u_{,y} + v_{,x} \end{Bmatrix} & = [B] & \begin{Bmatrix} u_1 \\ v_1 \\ u_2 \\ v_2 \\ \vdots \\ \vdots \end{Bmatrix} & \dots\dots\dots(13)
\end{matrix}$$

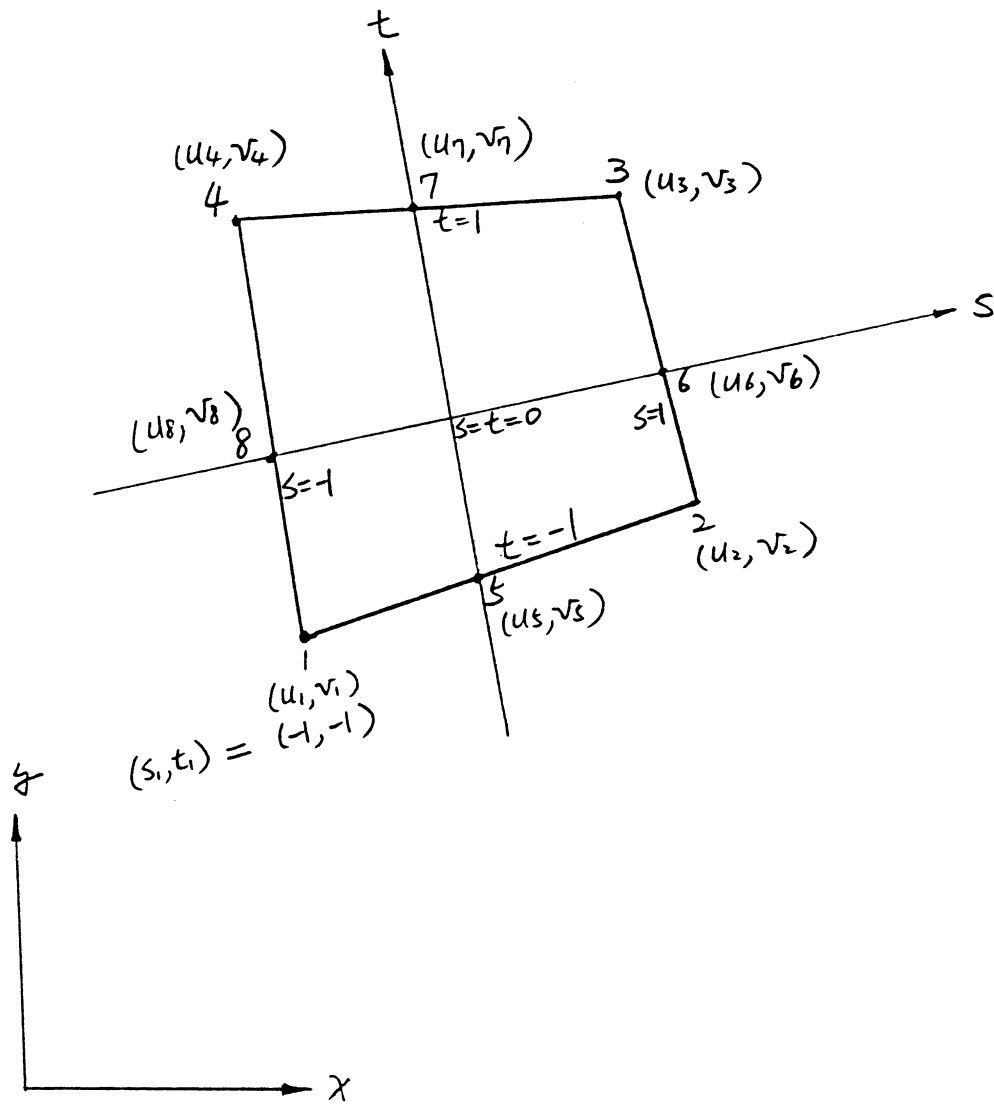


Figure 2 System Coordinates

in which $[B] = [B_1, B_2, \dots, B_8]$

with

$$B_i = \begin{bmatrix} N_{i,x} & 0 \\ 0 & N_{i,y} \end{bmatrix} \dots \dots \dots (14)$$

$$N_{i,y} \quad N_{i,x}$$

where u, v are the node displacements in the x, y directions.

N_i are the shape function of i 'th node of each element. As N_i is defined in terms of s and t it is necessary to change the derivatives to $,x$ and $,y$. Noting that

$$\begin{Bmatrix} N_{i,s} \\ N_{i,t} \end{Bmatrix} = \begin{bmatrix} x_{,s} & y_{,s} \\ x_{,t} & y_{,t} \end{bmatrix} \begin{Bmatrix} N_{i,x} \\ N_{i,y} \end{Bmatrix} = [J] \begin{Bmatrix} N_{i,x} \\ N_{i,y} \end{Bmatrix} \dots \dots \dots (15)$$

in which $[J]$ is the Jacobian matrix which can easily be evaluated by using three-by-three Gaussian quadrature. Noting that

$$[J] = \begin{bmatrix} N_{1,s} & N_{2,s} & \dots \dots \dots \\ N_{1,t} & N_{2,t} & \dots \dots \dots \end{bmatrix} \begin{bmatrix} x_1 & y_1 \\ x_2 & y_2 \\ x_3 & y_3 \\ \vdots & \vdots \\ \vdots & \vdots \\ \vdots & \vdots \end{bmatrix} \dots \dots \dots (16)$$

we can write

$$\begin{Bmatrix} N_{i,x} \\ N_{i,y} \end{Bmatrix} = [J]^{-1} \begin{Bmatrix} N_{i,s} \\ N_{i,t} \end{Bmatrix} \dots \dots \dots (17)$$

and thus calculate the expression for [Bi].

The only further change is to replace the element of area as

$$dx dy = \det [J] ds dt$$

and the limits of integration to -1 and 1 in both integrals.

3 - 3 Crack Tip Element

The standard eight-noded element of last section in an x y space which is transformed to a square in the s, t space with matrices at (+ 1, - 1) is considered. The behavior of the mid-side nodes as they are moved away from their usual positions (Figure 3) is of interest, and to simplify the mathematics just one of the sides is considered as a one-dimensional element. This element, which is shown in Figure 4, has nodes at s = -1, 0, + 1 and r=0, e , 2. The undistorted element corresponds to e=1 . The assumptions for transformation and displacement take the forms

$$\begin{aligned} r &= a_1 + a_2 s + a_3 s^2 \\ u &= b_1 + b_2 s + b_3 s^2 \end{aligned} \dots\dots\dots (18)$$

where ai and bi are constants and r = x/h.

$$\begin{Bmatrix} 0 \\ e \\ 2 \end{Bmatrix} = \begin{bmatrix} 1 & -1 & 1 \\ 1 & 0 & 0 \\ 2 & 1 & 1 \end{bmatrix} \begin{Bmatrix} a_1 \\ a_2 \\ a_3 \end{Bmatrix} = [T] \begin{Bmatrix} a_1 \\ a_2 \\ a_3 \end{Bmatrix} \dots\dots (19)$$

$$\begin{Bmatrix} a_1 \\ a_2 \\ a_3 \end{Bmatrix} = [T]^{-1} \begin{Bmatrix} e \\ \\ 2 \end{Bmatrix}$$

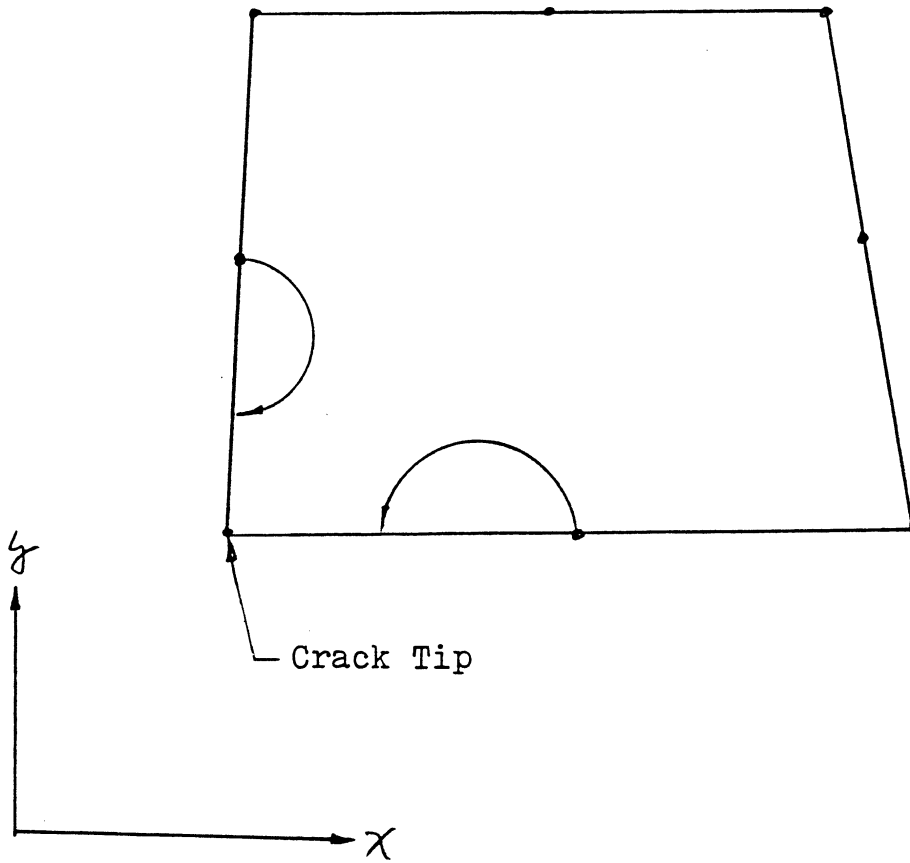


Figure 3 Distortion of an eight-noded element.

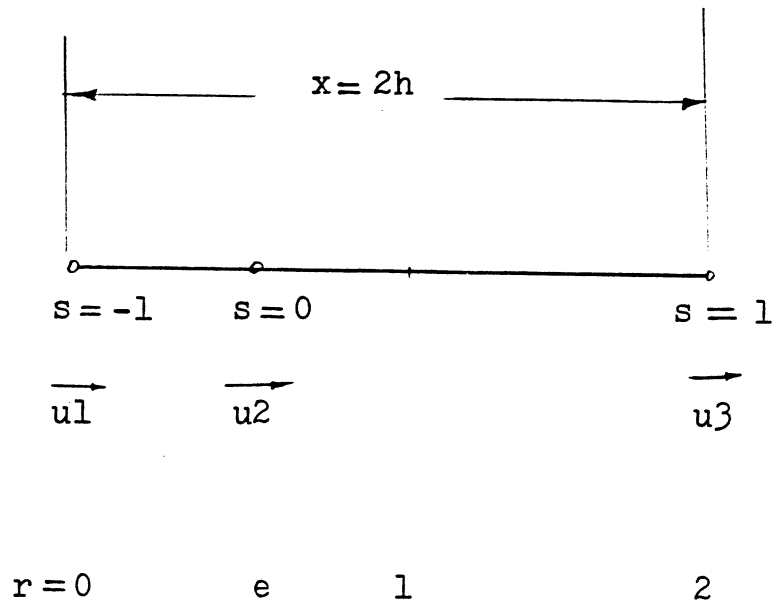


Figure 4 One dimensional distorted element.

Substitute a_1 , a_2 , and a_3 in equation (18)

$$r = a_1 + a_2 s + a_3 s^2 = e + s + (1 - e) s^2$$

$$\text{or } s^2 (1 - e) + s + (e - r) = 0 \dots\dots\dots (20)$$

Therefore,

$$s = \frac{-1 \pm \sqrt{1 - 4e + 4e^2 + 4(1 - e)r}}{2(1 - e)}$$

$$\frac{ds}{dr} = (1 - 4e + 4e^2 + 4(1 - e)r)^{-1/2} \dots\dots\dots (21)$$

This has a singularity when

$$r = \frac{(1 - 2e)^2}{4(e - 1)}$$

This singularity occurs at the $r = 0$ end of the element when $e = 1/2$.

This yields the following expressions for s , ds/dr and for u

$$s = -1 + \sqrt{2r} \quad , \quad ds/dr = (2r)^{-1/2}$$

since

$$\begin{matrix} b_1 & & u_1 & & u_2 \\ \{ b_2 \} = [T]^{-1} & \{ u_2 \} = & \{ & 1/2 (u_3 - u_1) & \} \dots\dots (22) \\ b_3 & & u_3 & & 1/2 (u_1 - 2u_2 + u_3) \end{matrix}$$

Substitute in equation (18)

$$u = u_1 \left[\frac{2 - 3\sqrt{2r} + 2r}{2} \right] + u_2 \left[-2r + 2\sqrt{2r} \right] + u_3 \left[\frac{2r - \sqrt{2r}}{2} \right] \dots (23)$$

It is the stresses that are of interest and these are proportional to the strains. In the one-dimensional element the longitudinal strain in

given by

$$\begin{aligned}
du/dr = & u_1 \left(1 - \frac{3}{2} (2r)^{-1/2} \right) + u_2 \left(-2 + 2 (2r)^{-1/2} \right) + \\
& u_3 \left(1 - \frac{1}{2} (2r)^{-1/2} \right) \dots\dots\dots (24)
\end{aligned}$$

Equation (24) clearly shows that the singularity is of the order $r^{-1/2}$ as required by the theoretical solutions. This suggests a simple idea to model the area near crack tip; when elements with one mid-side node are used at crack tip the mid-side nodes should be moved from their usual position at the center of each side to the 1/4 position as shown in Fig. 5.

Note that these elements at the crack tip are not in any way special. A standard procedure to compute general stiffness and mass matrices for isoparometric element is used throughout the mesh.

3 - 4 Consistent Mass Matrix

The consistent mass matrix for an element is established in the same way as the generalized stiffness matrix [k] and it is given by

$$[m] = \iint [G]^T [C] [G] dx dy \dots\dots\dots (25)$$

where

$$[C] = \begin{bmatrix} 1 & 0 \\ 0 & 1 \end{bmatrix}$$

$$[G] = [G_1, G_2, G_3, \dots\dots\dots, G_8]$$

$$G_i = \begin{bmatrix} N_i & 0 \\ 0 & N_i \end{bmatrix} \quad i = 1, 2, \dots\dots\dots 8$$

we can rewritten [m] in terms of element coordinates s,t

$$[m] = \int_{-1}^1 \int_{-1}^1 [G]^T [C] [G] \det J ds dt \dots\dots\dots (26)$$

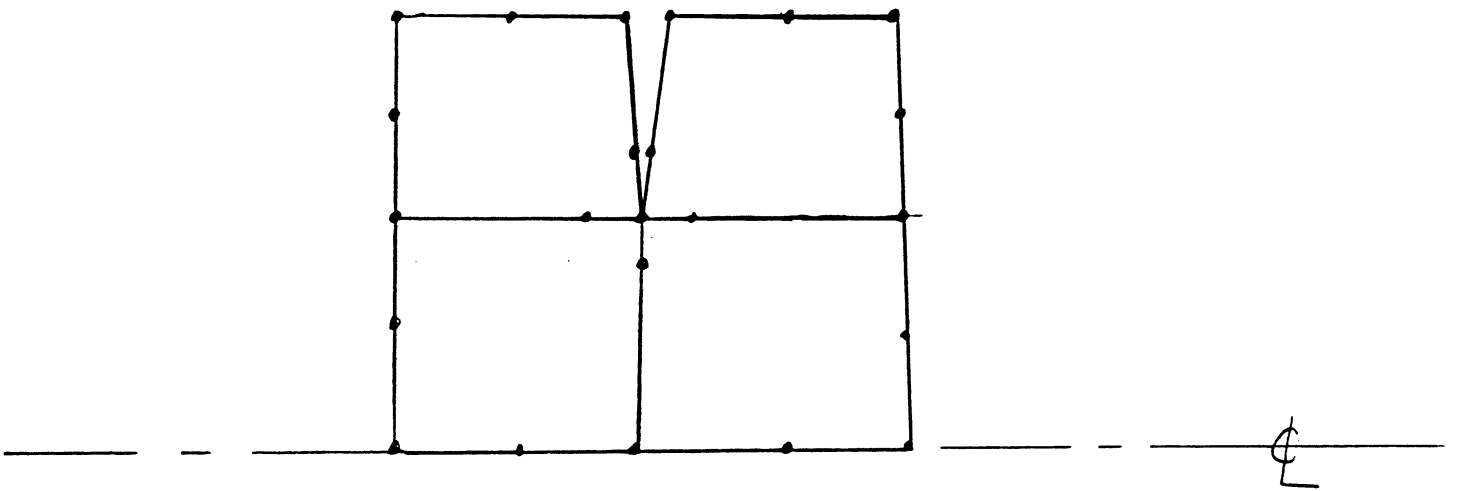


Figure 5 Distortion of Elements in the Region of Singularity.

By assembling finite elements and applying to kinematic boundary conditions, the free vibration eigenvalue problem of beam may be written as

$$\omega^2 [M] \{u\} = [K] \{u\} \dots\dots\dots (27)$$

The assemblage processes to obtain the system stiffness matrices [K], and system mass matrix [M] are symbolically

$$(K, M) = \sum_{i=1}^n (k_i, m_i) \dots\dots\dots (28)$$

where the matrices [k], and [m] are for the ith element and summation goes over all n element in the assemblage.

CHAPTER 4 RESULTS AND DISCUSSION

Using the present finite element approach and theoretical formulation of chapters 2 and 3, the free vibrations of rectangular cross section cracked beam with simply supported are studied. The frequencies and deflection shapes are obtained for the first three modes by finite element method and then compared to the theoretical as well as experimental results for the fundamental mode only. The first three mode shapes of cracked beam are plotted to examine the difference between the ones of the corresponding uncracked beam.

The beam's material properties are listed in Table 1.

Figure 6 shows the finite element gridwork that is used for the simply supported cracked beam.

The natural frequencies and mode shapes in flexure of the uncracked beam were first obtained and comparison with the Bernoulli-Euler theory results are listed in Table 2. Then cracks symmetric with respect to the neutral axis and normal to it were made on the upper and lower beam surfaces at midlength. The natural frequencies and mode shapes of the beam for the cracks depth of $1/3$, $1/2$, and $2/3$ total of the beam were computed. Finite element, experimental, and analytical results for the fundamental mode are compared in Figure 7. They are presented in the form of the frequency ratio (FR), that is the ratio of the frequency of the cracked beam to that of the uncracked, against the crack depth ratio (CR), i.e. the ratio of the depth of crack to the half depth of the beam thickness.

Table 1 Properties of The Beams

E	4.1472	$\times 10^3$	psi
ν	0.3		
Density	2.4	$\times 10^{-4}$	lb-sec ² /in ⁴

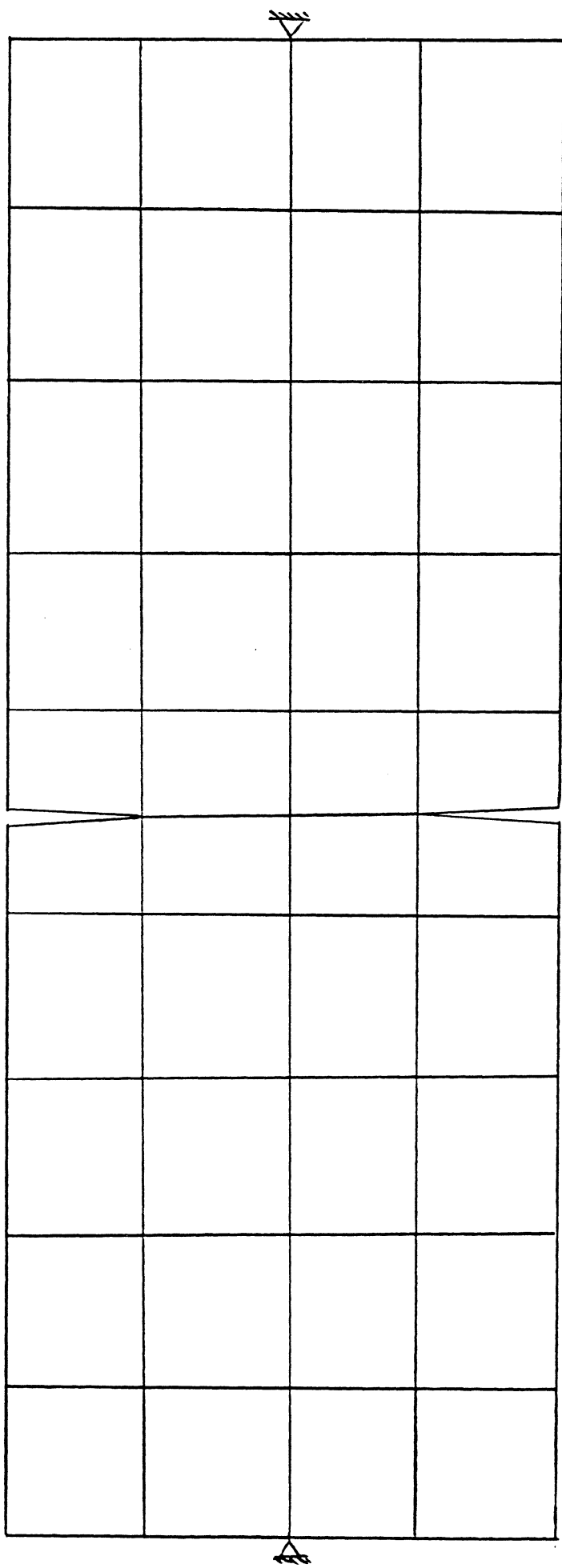


Figure 6 Finite Element Gridwork for a Simply Supported cracked beam

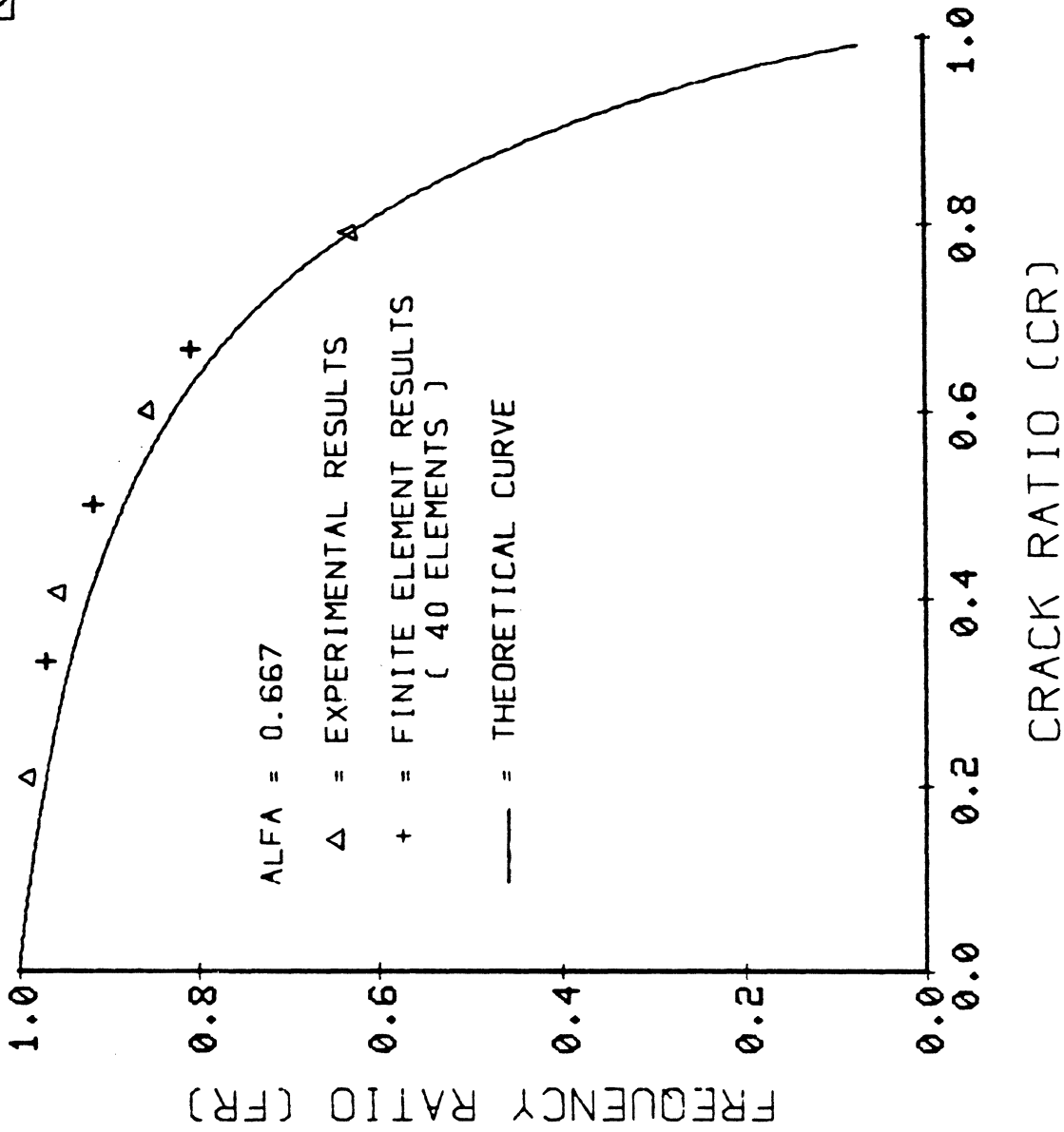


FIGURE 7 COMPARISON OF FINITE ELEMENT, EXPERIMENTAL AND THEORETICAL VALUES OF FREQUENCY RATIO. (FIRST MODE)

From Table 2 and Figure 7, it is obviously shown that the finite element results agree well with the experimental results as compared to analytical results. Therefore, one can use the finite element results to determine the parameter α for the theoretical expression of equation (10). Examples are shown in Figure 8. The theoretical curves 1,2,3,and 4 were plotted for various of parameter α . The best chosen of parameter to given agreement with the finite element results is 0.667 of curve 1 which is the same value obtained from experimental results.

In Figures 9-17 the first three normal mode shapes of cracked beam with various crack ratios are plotted and compared to uncracked beam. It can be seen from these figures that the changes of the first and third mode shapes between cracked and uncracked beams are significant. But the second mode shapes are almost the same for uncracked and cracked beams, for all crack ratios studied. The reasons behind these are because the positions of the cracks in the present study are located at mid-span of the beam. Therefore, the stress singularity phenomenon occurs severely when the cracks under compress or tension in the first or third mode vibrations. Since the cracks at the mid-span are not under severe compress or tension at the second mode, the strain in neutral axis direction is almost zero except very small in-plane strain occurs due to the in-plane displacement. Therefore, stress singularity phenomenon vanish and the cracks does not affect the eigenfrequency and eigenmode for the second mode vibration.

Tables 3-5 show the stress level for each element. Stress singularity phenomenon occurs at the elements near crack tip for the first and third modes. Almost the same stress level of each element between cracked and uncracked beams is observed for the case of second mode.

TABLE 2
COMPARISON BETWEEN CRACKED AND UNCRACKED BEAM

UNCRAKED BEAM

	Theoretical		Finite Element	
	Natural frequency (Hz)		Natural frequency (Hz)	Total strain energy
1st mode	9.87		9.846	198
2rd mode	39.5		39.100	807
3rd mode	88.9		87.191	1840

CRACKED BEAM

	Theoretical		Finite Element		
	CR	ER	Natural frequency (Hz)	ER	Total strain energy
1st mode	1/3	.9435	9.5497	.9699	192
	1/2	.8840	9.0300	.9171	184
	2/3	.7760	7.9596	.8040	173

*** Note: CR : crack ratio , ER : frequency ratio

CRACKED BEAM

	Theoretical		Finite Element		
	CR	FR	Natural frequency (Hz)	FR	Total strain energy
2rd mode	1/3		39.100	1.0	805
	1/2		39.100	1.0	804
	2/3		39.100	1.0	803
3rd mode	1/3		84.7136	.9715	1600
	1/2		80.9534	.9284	1400
	2/3		74.9430	.8595	1220

=====

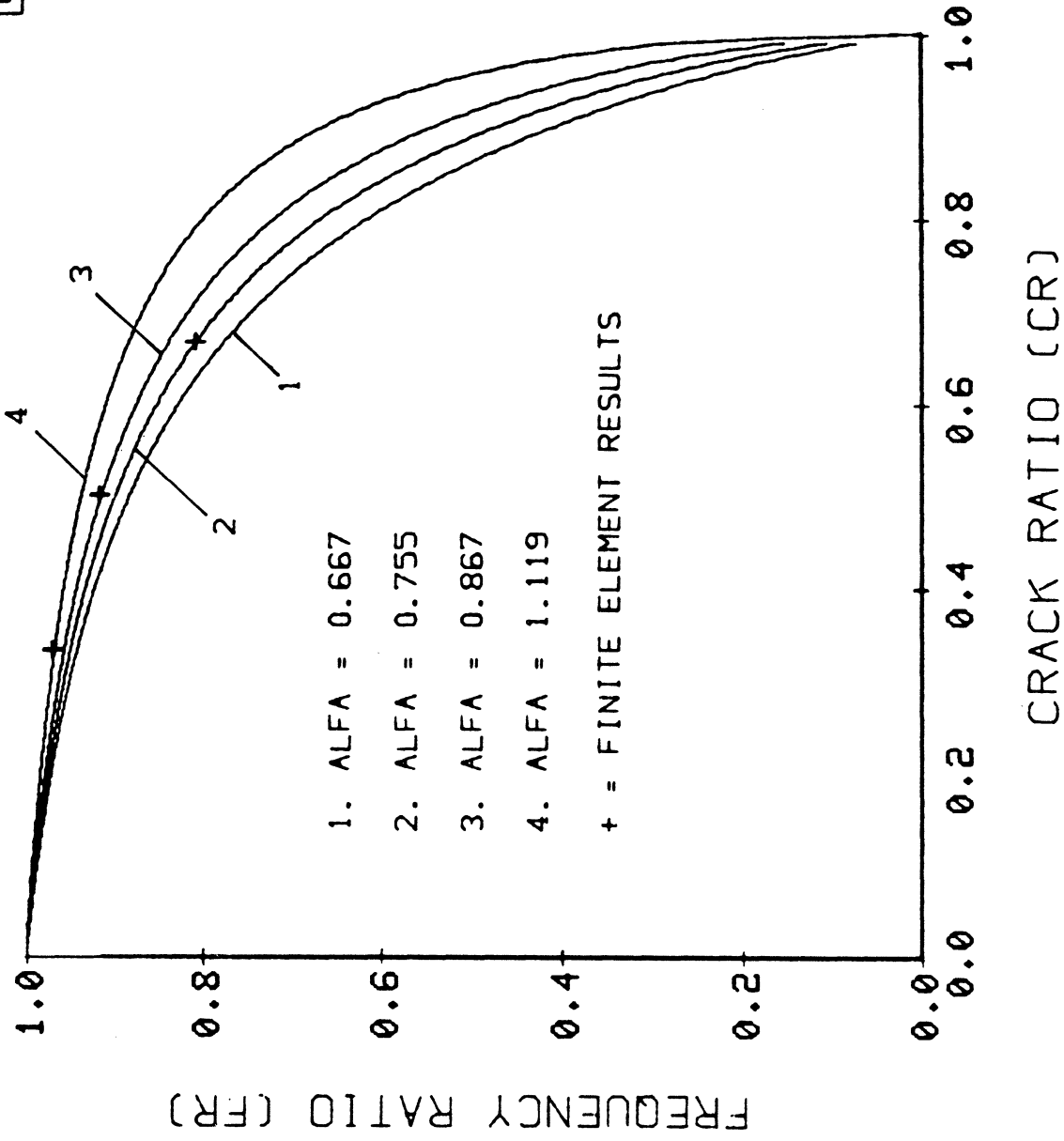


FIGURE 8 THEORETICAL CURVE DUE TO VARIOUS ALFA (FIRST MODE).

— MODE SHAPE OF UNCRACKED BEAM

- + - MODE SHAPE OF CRACKED BEAM

NOTE CRACK RATIO (CR=1/3)

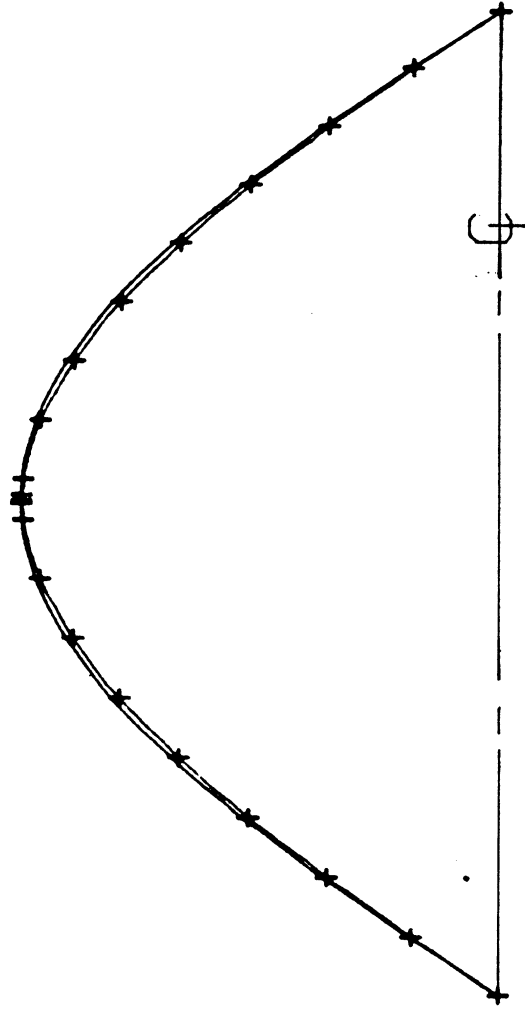


FIGURE 9 FIRST MODE SHAPES OF UNCRACKED AND CRACKED BEAMS.

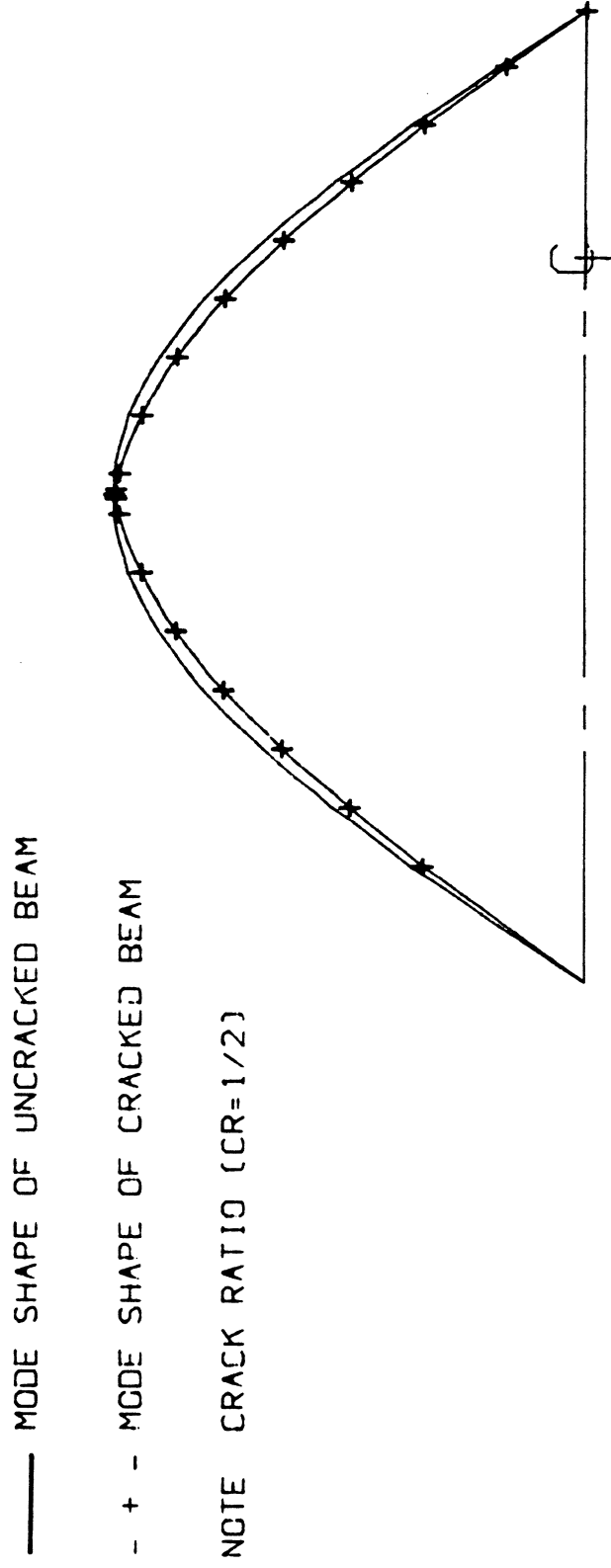


FIGURE 10 FIRST MODE SHAPES OF UNCRACKED AND CRACKED BEAMS.

— MODE SHAPE OF UNCRACKED BEAM

- + - MODE SHAPE OF CRACKED BEAM

NOTE CRACK RATIO (CR=2/3)

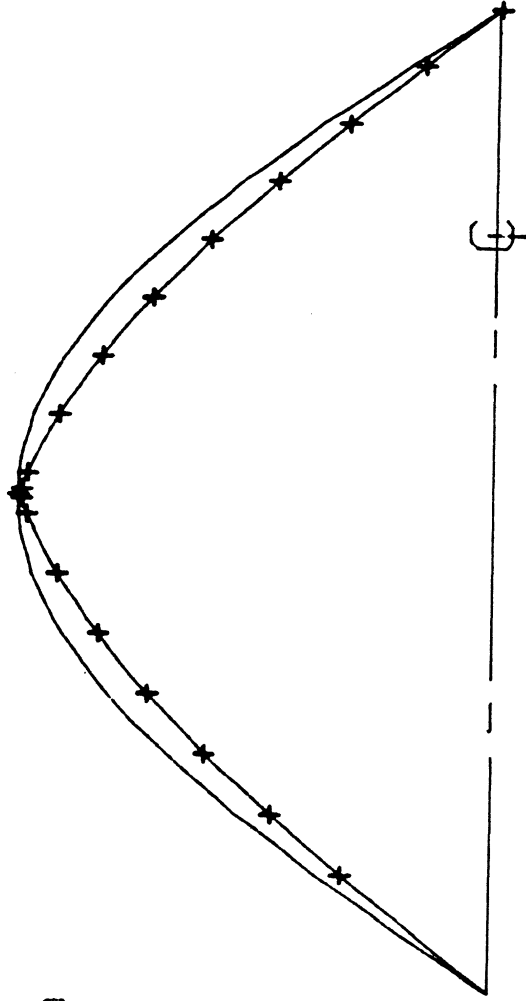


FIGURE 11 FIRST MODE SHAPES OF UNCRACKED AND CRACKED BEAMS.

C:

— MODE SHAPE OF UNCRACKED BEAM

- + - MODE SHAPE OF CRACKED BEAM

NOTE CRACK RATIO (CR=1/3)

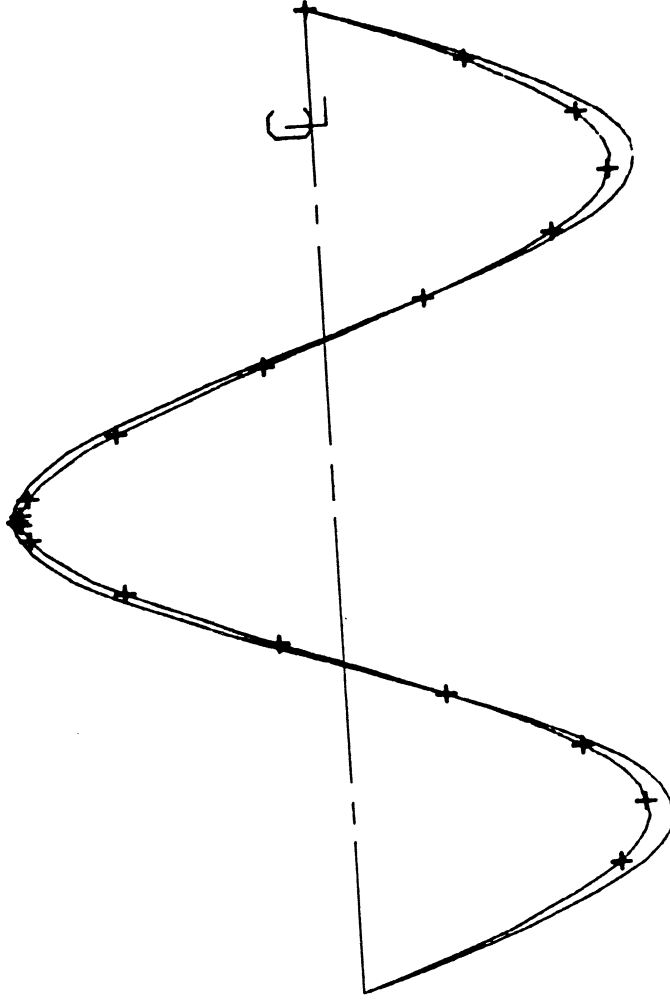


FIGURE 12 THIRD MODE SHAPES OF UNCRACKED AND CRACKED BEAMS.

— MODE SHAPE OF UNCRACKED BEAM

- + - MODE SHAPE OF CRACKED BEAM

NOTE CRACK RATIO (CR=1/2)

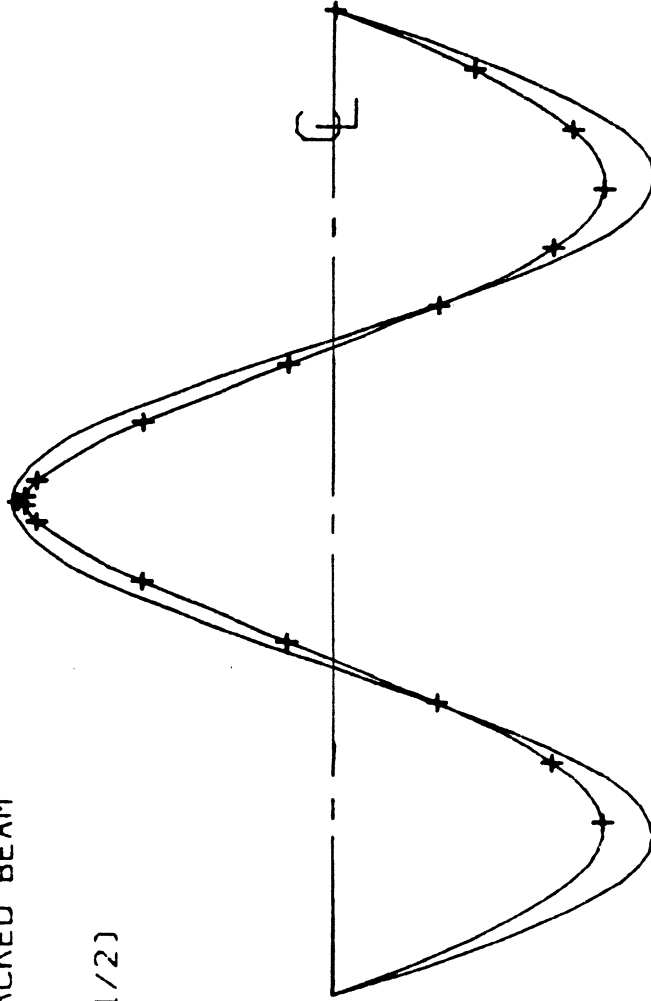


FIGURE 13 THIRD MODE SHAPES OF UNCRACKED AND CRACKED BEAMS.

— MODE SHAPE OF UNCRACKED BEAM

- + - MODE SHAPE OF CRACKED BEAM

NOTE CRACK RATIO (CR=2/3)

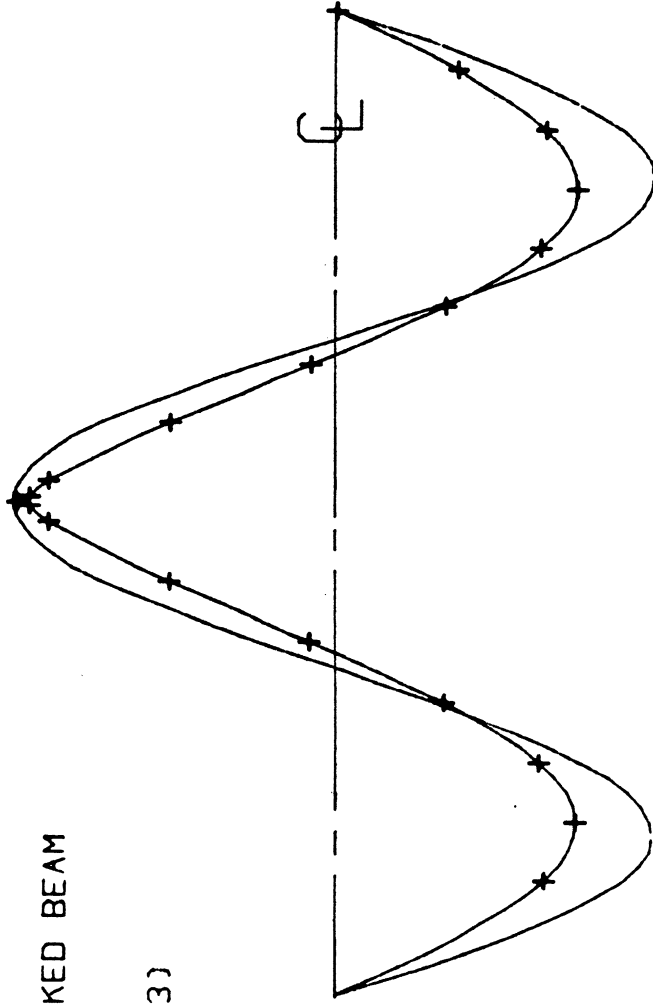


FIGURE 14 THIRD MODE SHAPES OF UNCRACKED AND CRACKED BEAMS.

C:

GRAF

— MODE SHAPE OF UNCRACKED BEAM

- + - MODE SHAPE OF CRACKED BEAM

NOTE CRACK RATIO (CR=1/3)

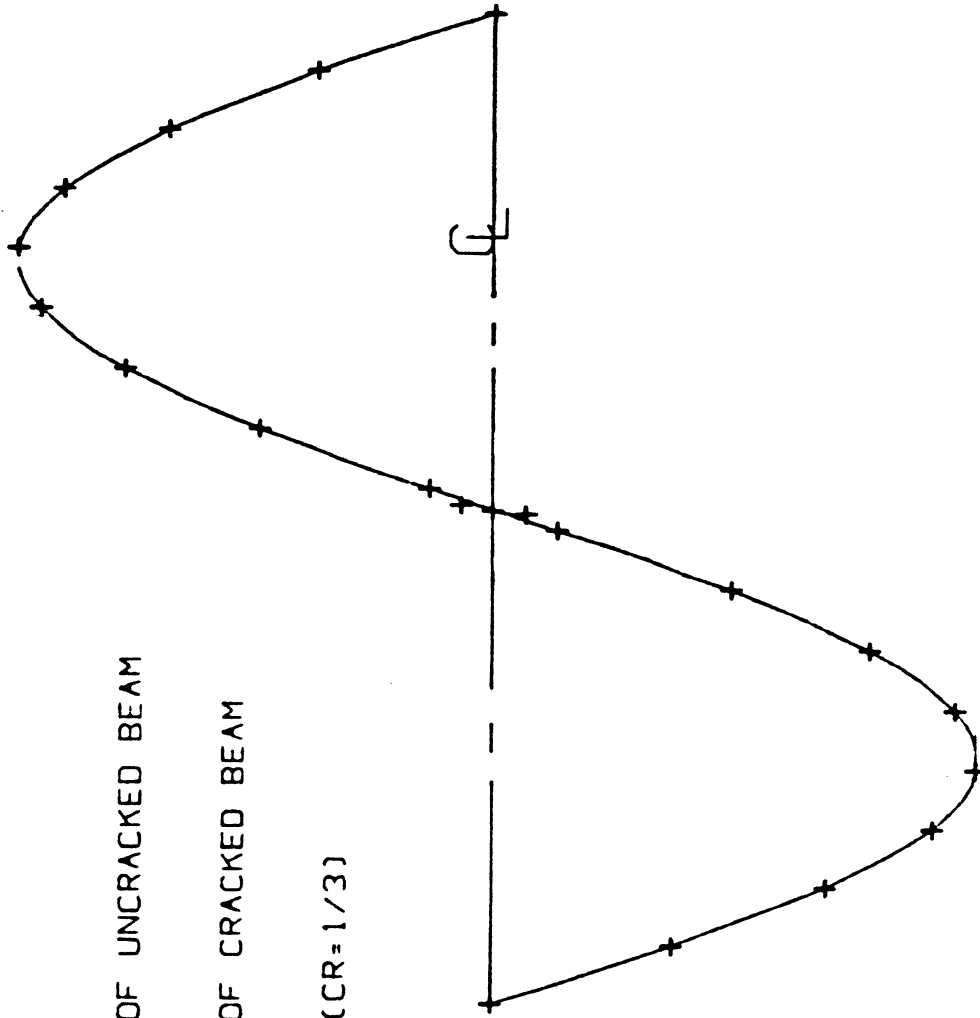


FIGURE 15 SECOND MODE SHAPES OF UNCRACKED AND CRACKED BEAMS.

— MODE SHAPE OF UNCRACKED BEAM

- + - MODE SHAPE OF CRACKED BEAM

NOTE CRACK RATIO (CR=1/2)

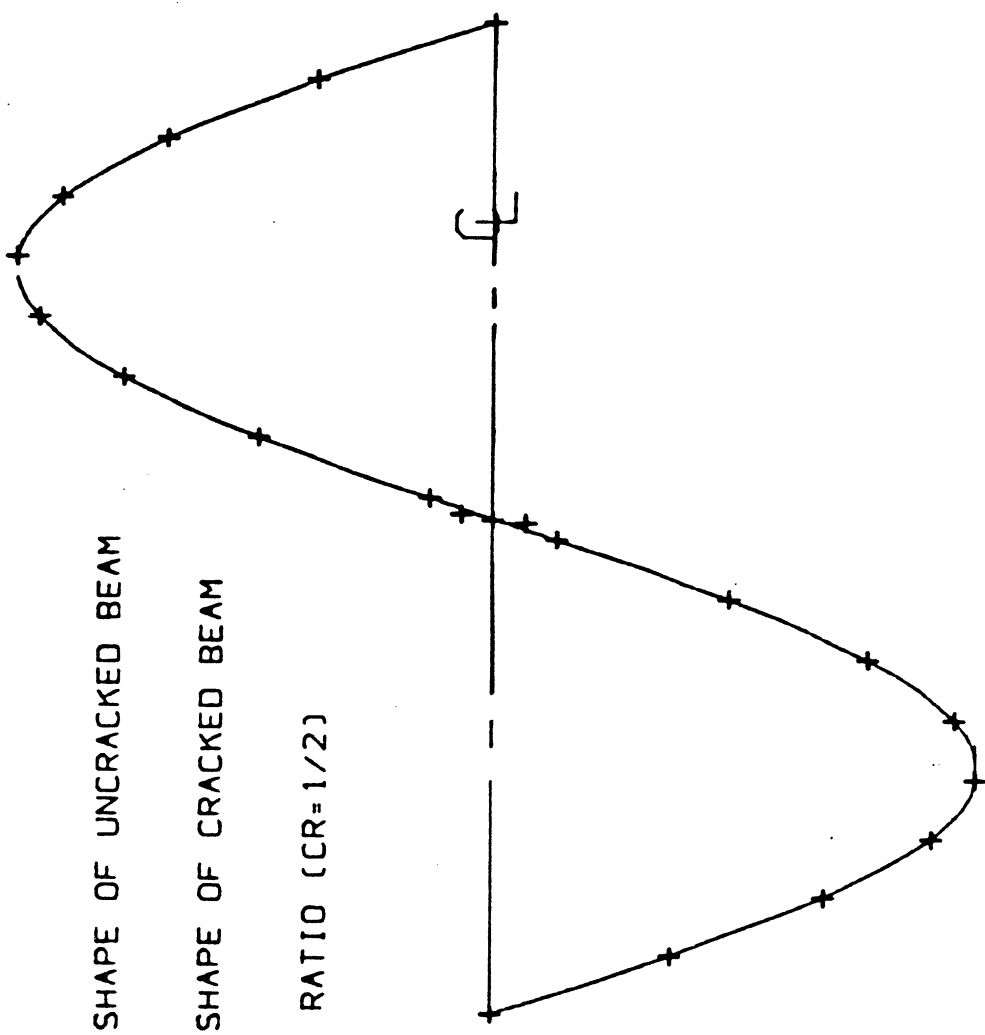


FIGURE 16 SECOND MODE SHAPES OF UNCRACKED AND CRACKED BEAMS.

GRAF

— MODE SHAPE OF UNCRACKED BEAM

- + - MODE SHAPE OF CRACKED BEAM

NOTE CRACK RATIO (CR=2/3)

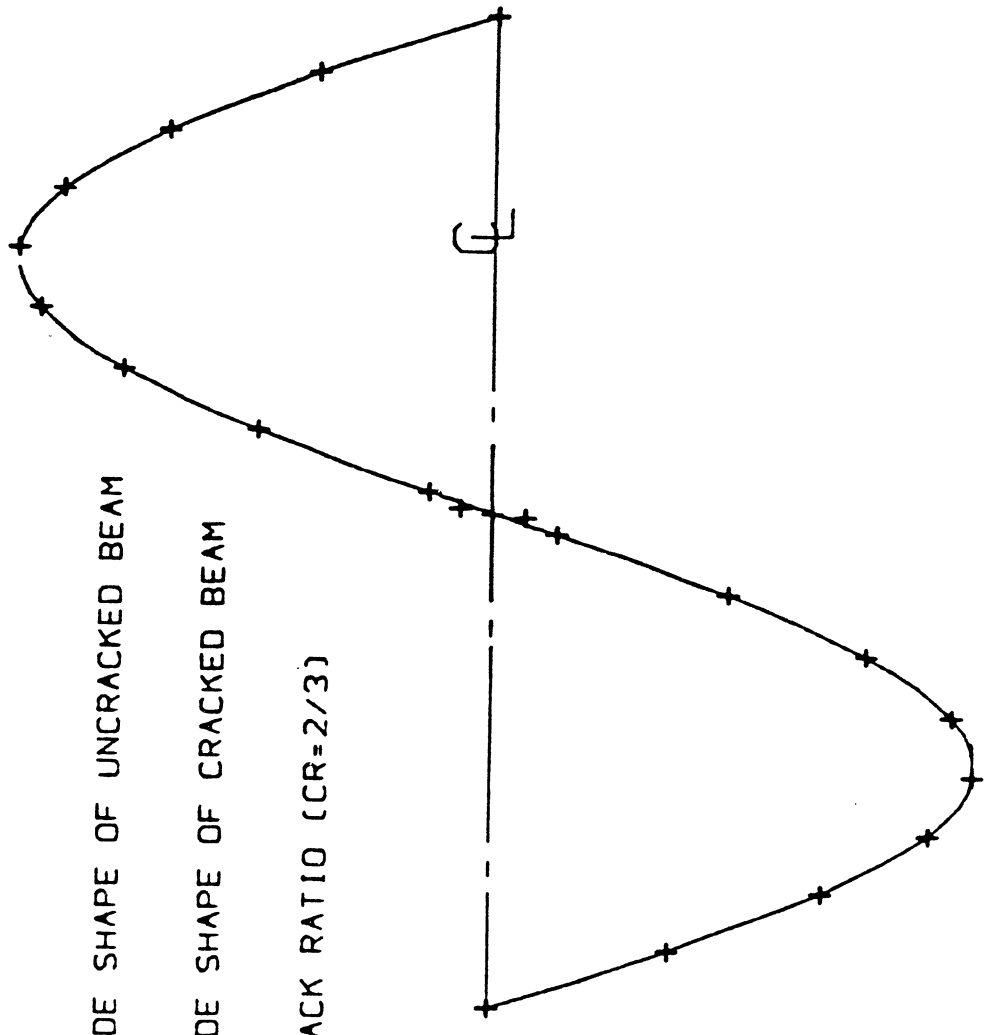


FIGURE 17 SECOND MODE SHAPES OF UNCRACKED AND CRACKED BEAMS.

Table 3 Normal Stress of each element for the case of $CR = 1/2$
 (First Mode)

line
of
symmetry

18.9	54.0	81.7	98.2	110.0
6.29	17.9	27.2	33.0	181.0
- 6.29	-17.9	-27.2	-33.0	-181.0
- 18.9	-54.0	-81.7	-98.2	-110.0



Table 4 Normal stress of each element for the case of $CR \approx 1/2$

(Second Mode)

line
of
symmetry

-180.0	-442.0	-465.0	-238.0	-257.0
- 59.5	-146.0	-154.0	- 78.9	-77.3
59.5	146.0	154.0	78.9	77.3
180.0	442.0	465.0	238.0	257



Table 5 Normal stress of each element for the case of $CR=1/2$

(Third Mode)

line
of
symmetr

-435.0	-842.0	-370.0	436.0	767.0
-142.0	-275.0	-121.0	145.0	1260.0
142.0	275.0	121.0	-436.0	-1260.0
435.0	842.0	370.0	-145.0	-767.0

CHAPTER 5

CONCLUSIONS AND SUGGESTIONS FOR FUTURE RESEARCH

A finite element approach has been presented for the prediction of changes in eigenfrequencies and eigenmodes due to cracks of a beam. Compared to an analytical method, the finite element method is easy to work with since it uses information which is mostly available, does not need any geometrical and material assumptions, and can be easily extended to other geometries, boundary conditions and various crack ratios. However, the finite element approach is quite expensive if mesh refined is required. A superelement can be applied to the cracked beam studies in order to reduce the computational cost. The idea is to model the crack tip area by using one or several superelements and applying two-node beam element for the rest of the beam. A trigular transition element is then necessary need to be used for connection between superelement and two-node beam element.

Examples treated are for crack ratio values of $1/3$, $1/2$, and $2/3$ with simply supported boundary conditions. The present finite element results are found to be in good agreement with the theoretical as well as experimental solutions. Both eigenfrequencies and mode shapes have severe change for the odd modes in the case of a pair of cracks located at mid-span of the beam.

The theoretical results depend on the value of parameter α which is chosen based on experiment results can also be determined by present finite element approach.

FUTURE STUDIES SHOULD INCLUDE THE FOLLOWING PROBLEMS:

- (1) The singularity element [Fig. 17(a)] used in this project displays the $1 / \sqrt{r}$ stress field only along its edges, therefore, other singularity elements are suggested for future studies. A six-node triangular element [Fig. 17(b)] and A nine-node quadrilateral element [Fig. 17(c)] display more the $1 / \sqrt{r}$ stress field by distorting three edges in stead of two edges of the present finite element approach. Another type of singularity element was proposed by Tracey, Cook [11] and Akin [12]. The four isoparametric quadrilateral element is considered first and it is verified that simplex triangular element is obtainable by collapsing one side (say 1-4) of the quadrilateral as shown in Figure 18(a). It can be easily shown that the cartesian coordinates x, y of a generic point q in the triangle are expressed parametrically as

$$\begin{aligned} x - x_1 &= \left[\frac{1 - t}{2} (x_2 - x_1) + \frac{1 + t}{2} (x_3 - x_1) \right] \\ y - y_1 &= \left[\frac{1 - t}{2} (y_2 - y_1) + \frac{1 + t}{2} (y_3 - y_1) \right] \end{aligned} \quad \dots\dots (27)$$

$$\text{where } s = -1 + 2\rho \quad \text{or} \quad \rho = \frac{1 + s}{2}, \quad 0 \leq \rho \leq 1$$

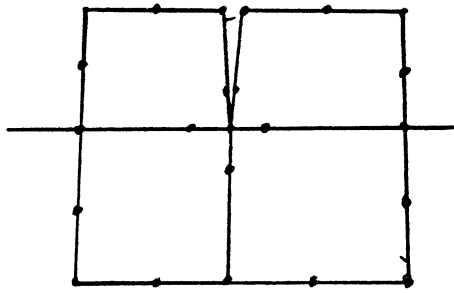
Original displacement fields

$$u = 0.25 (1 - s) (1 - t) u_1 + 0.25 (1 + s) (1 - t) u_2 + 0.25 (1 + s) (1 + t) u_3 + 0.25 (1 - s) (1 + t) u_4$$

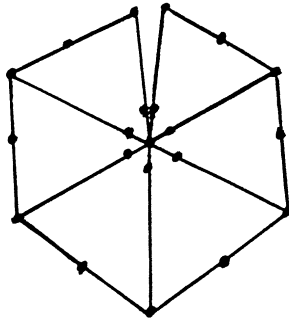
can be rewritten as

$$u = u_1 + 0.5 (1 - t) \rho^\lambda (u_2 - u_1) + 0.5 (1 + t) \rho^\lambda (u_3 - u_1)$$

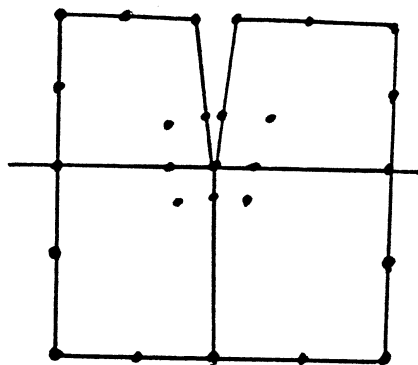
$$u_1 = u_4$$



(a)



(b)



(c)

Figure 18 Various Crack tip Elements.

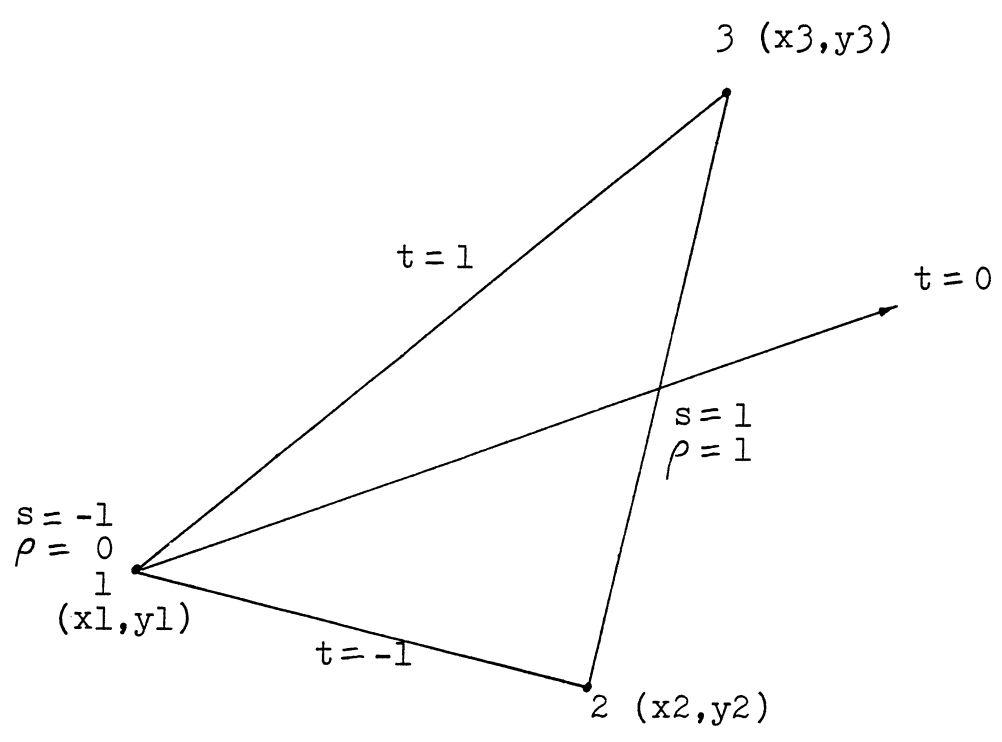


Figure 19 Simplex Triangular Element.

where $\lambda = -1/2$ or other values which are determined by different crack tip shapes.

The displacement field of Akin [11] for the three-node triangular element is expressed as follows:

$$u = (1 - A^{1-g}) u_1 + \frac{N_2}{A^g} u_2 + \frac{N_3}{A^g} u_3$$

$$\text{with } A = 1 - N_1, \quad 1 - g = \lambda$$

where N_1, N_2 represent the shape functions of the standard element.

These power ρ^λ type singularity element can provide uniform singularity stress field.

- (2) Vibration of cracked shafts or beams loaded laterally by their own weight, or static and dynamic loads, for a crack closing at positions where compressive stresses occur at the location of crack introduces time varying factor into the equation of motion. In this case, nonlinear (piecewise linear) characteristics are included in the equation of motion. This will bring difficulty to the solution of the equation of motion.

REFERENCES

1. H. Liebowitz, H. Vanderveldt and D.W. Harris, " Carrying capacity of notched column", Int. J. Solids Structures, Vol.3, P.489-500 1967.
2. H. Liebowitz and W.D.S. Claus, Jr., "Failure of Notched columns", Engng Fracture Mech. Vol.1, P.379-383, 1968.
3. H. Okamura, "A cracked column under compression", Engng Fracture Mech., Vol.1, p.547, 1969.
4. J.R. Rice, and N. Levy, "The part-through surface crack in an electric plate", J. Appl. Mech. P.185, 1972.
5. A.D. Dimarogonas, Vibration Engng , WEST, St. Paul, 1976.
6. T.G. Chondros and A.D. Dimarogonas, "Identification of cracks in welded joints of complex structures", J. Sound Vibr. Vol.69, p.531-538, 1980.
7. S. Christides and A.D.S.Barr, "One-Dimensional Theory of Cracked Bernoulli-Euler Beams", Int. J. Mech. Sr., Vol. 26, p.639-648, 1984.
8. Hai-Chang Hu, "On some variational principals in the theory of elasticity and plasticity", Scientia Sinica, Vol.4, P.33-55, 1955.
9. K. Washizu, "Varitional Methods in elasticity and plasticity", 3rd Edn. Pergamon Press, Oxford, 1982.
10. A.D.S.Barr, "An extension of the Hu-Washizu variational principle in linear elasticity for dynamic problems", Trans. ASME J. Appl. Mechs. Vol.33(2), P. 465, 1966.
11. D.M. Tracey and T.S.Cook, "Analysis of power type singularities using finite elements", Int. J. Num. Meth. Engng, Vol.11, P. 1225-1233, 1977.
12. J.E.Akin, "The generation of elements with singularities", int. J. num. Meth. Engng Vol.10, p.1249-1259, 1976.